

The ParMRC system: molecular mechanisms of plasmid segregation by actin-like filaments

Jeanne Salje, Pananghat Gayathri and Jan Löwe

Abstract | The ParMRC plasmid partitioning apparatus is one of the best characterized systems for bacterial DNA segregation. Bundles of actin-like filaments are used to push plasmids to opposite poles of the cell, whereupon they are stably inherited on cell division. This plasmid-encoded system comprises just three components: an actin-like protein, ParM, a DNA-binding adaptor protein, ParR, and a centromere-like region, *parC*. The properties and interactions of these components have been finely tuned to enable ParM filaments to search the cell space for plasmids and then move ParR-*parC*-bound DNA molecules apart. In this Review, we look at some of the most exciting questions in the field concerning the exact molecular mechanisms by which the components of this self-contained system modulate one another's activity to achieve bipolar DNA segregation.

Walker A protein

Protein that contains a Walker A motif (GXXXGKT; where X is any amino acid), and is involved in the nucleotide binding of many ATP-requiring enzymes.

Tubulin

Basic subunit of microtubules. Tubulin comes in two forms, α -tubulin and β -tubulin, which form heterodimers that make up microtubules.

Many bacterial plasmids are maintained at low copy number (~1–5 copies per chromosome equivalent). To prevent plasmid loss at cell division, plasmids have evolved active segregation mechanisms that are loosely analogous to the spindle apparatus in eukaryotic cells^{1–3}. These segregation machineries involve a small number of components, and they are remarkable for the efficiency with which these components interact with and modulate the activity of one another to achieve plasmid motility. Plasmid segregation systems usually function by separating pairs or clusters of newly replicated plasmid molecules and then moving an equal number to opposite halves of the host cell to ensure that they will be equally inherited by both daughter cells on cell division.

Three major classes of segregation system have been identified to date for low-copy-number plasmids⁴. Although these are composed of apparently unrelated proteins, they are unified by a common overall genetic organization, similar to that of the *parMRC* locus shown in FIG. 1a. Each system has three components: a nucleotide-driven motor protein, a small DNA-binding adaptor protein and a centromere-like DNA region to which the adaptor binds. The motor protein defines the class of segregation system and can be described as ParA-like (type I; BOX 1), ParM-like (type II) or TubZ-like (type III; BOX 1). The motor proteins form nucleotide-dependent cytomotive filaments⁵, with the ParA family being driven by a deviant Walker A protein, the ParM family comprising

dynamic actin-like filaments and the TubZ family consisting of dynamic filaments that have a tubulin-like fold at the monomer level⁶. A potential fourth class of plasmid segregation system has recently been described and seems to require just a single protein for segregation⁷.

The *parMRC* locus was originally isolated from the large, low-copy-number, multiple-antibiotic-resistant plasmid R1 from *Escherichia coli*⁸, and it is currently the best characterised active plasmid segregation system. The fundamental molecular mechanism for DNA segregation by *parMRC* is thought to be based on bundles of actin-like ParM filaments that push ParR-*parC*-bound plasmids to opposite poles of the cell by a mechanism of insertional polymerisation⁹ (FIG. 1b,c). ParM filaments are dynamically unstable unless they are capped by the plasmid-bound ParR-*parC* nucleoprotein complex, and they thus use cycles of growing and shrinking to search the cell space for plasmids¹⁰. Only when they are capped by a ParR-*parC* complex at both ends do the filaments become stabilized; their subsequent bidirectional elongation ensures that the filament-bound plasmids move to opposite poles.

Several closely related ParMRC systems have been identified on plasmids from both Gram-positive and Gram-negative bacteria. Although most experiments have been carried out on the original *E. coli* R1 system, an increasing amount of mechanistic work has focused on components of the ParMRC systems from

Medical Research Centre
Laboratory of Molecular
Biology, Hills Road,
Cambridge CB2 0QH, UK.
Correspondence to J.L.
e-mail: jjl@mrc-lmb.cam.ac.uk
doi:10.1038/nrmicro2425

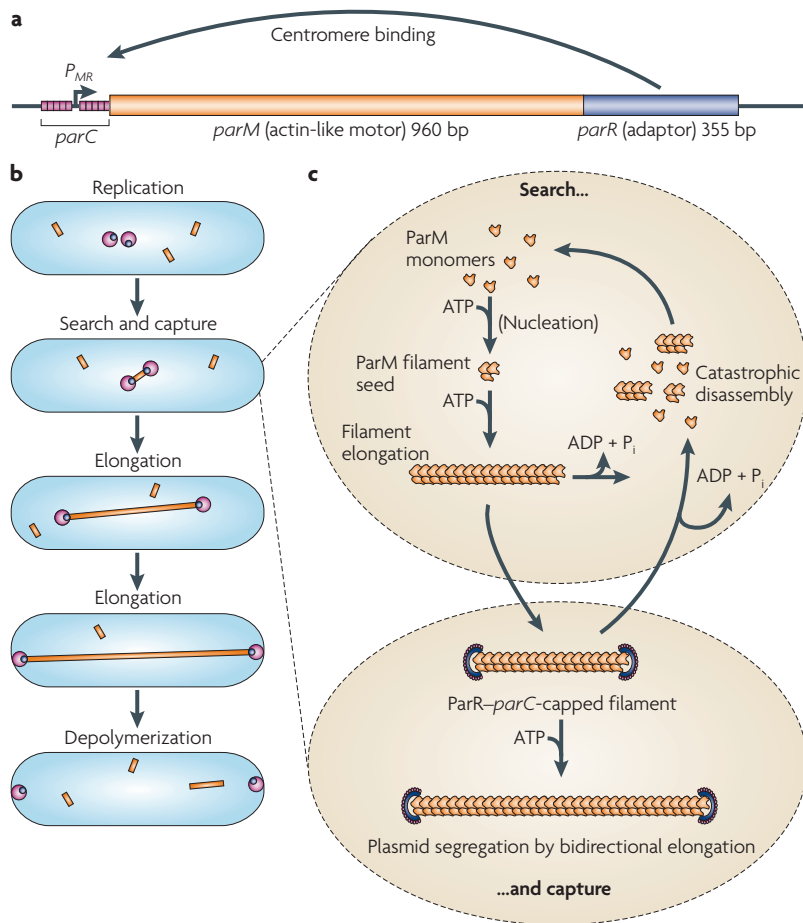


Figure 1 | An overview of the plasmid R1-encoded ParMRC plasmid segregation system. **a** | The *parMRC* operon. The centromere, *parC*, is composed of two blocks of five short repeats, which are interrupted by a 39 bp region containing the promoter for *parM* and *parR* (P_{MR}). *ParR*, an adaptor protein, binds to *parC* and represses transcription. **b** | Plasmid segregation by dynamic *ParM* filaments in cells. Plasmids are shown in pink, *ParR* in blue and *ParM* in orange. **c** | Search and capture: the molecular mechanism of plasmid segregation by *ParM*. *ParM* forms short filaments in the presence of ATP, which either undergo catastrophic disassembly following ATP hydrolysis to ADP plus inorganic phosphate (P_i), or become capped by a *ParR*–*parC* complex and undergo stable bipolar elongation.

Filamentous actin

Flexible, helical polymer of G-actin monomers that is 5–9 nm in diameter. This polymer is polar, displaying a plus end and a minus end.

Microtubule

Hollow tube, 25 nm in diameter, that is formed by the lateral association of 13 protofilaments, which are themselves polymers of α -tubulin and β -tubulin subunits.

the *Staphylococcus aureus* plasmid pSK41 and the *E. coli* plasmid pB171 (REFS 11–13). Two recent reports identified several other plasmid segregation systems that are driven by dynamic actin-like filaments. These actin homologues are as distantly related to *ParM* as they are to actin in terms of primary sequence, and there are reports that certain aspects of the structure and dynamics of these filaments may differ from those of *ParM*^{14–17}. However, it is reasonable to assume that the overall principle of coupling filament dynamics to an adaptor-centromere complex to achieve DNA motility is conserved, along with the actin-like fold of the motor element.

There are three areas of active research that aim to dissect and validate the insertional polymerization model for R1 *ParMRC*-mediated plasmid DNA segregation. The first area of research concerns the exact conformation and arrangement of *ParM* in its polymerized and monomeric states, and how these explain the dynamic behaviour of

ParM filaments. The second area aims to elucidate the details of the *ParR*–*parC* interaction with *ParM* filaments and the molecular mechanism by which this interaction results in filament stabilization and elongation. Finally, the third area covers how the *ParMRC* segregation system functions in its cellular environment and whether there are any additional, host-encoded factors or signals that are required to mediate accurate DNA segregation. Here, we review the current state of understanding in these three areas and describe the outstanding challenges in and beyond these areas of research. We also compare the structural and dynamic properties of *ParM* filaments with those of the two major eukaryotic cytoskeletal filaments, filamentous actin (F-actin) and microtubules.

Dynamics and structure of *ParM* filaments

Cytomotive filaments. Protein filaments can lead to molecular movement and force generation in one of two ways: by providing a track for other proteins to move or ratchet along, or by attaching their ends to a structure and pushing or pulling it as a result of filament growth or shrinkage. This second mode of action distinguishes dynamic filaments from static oligomeric assemblies and is achieved by coupling nucleotide binding and hydrolysis to polymerization. Such dynamic behaviour of cytoskeletal filaments has been described as ‘cytomotive’ (REF. 5), and it has been proposed that cytomotive filaments might have constituted the original cytoskeleton, with the adaptation to serve as tracks for motor proteins having evolved as a result of the demand for greater complexity in eukaryotic cells⁵. Indeed, although actin and microtubules use both motor proteins and dynamic reorganization to transport cargo and reorganize cellular structures, no motor proteins have been found in bacterial cells to date, and the bacterial cytoskeleton is instead composed of several dynamic, cytomotive filaments, including the chromosomally encoded tubulin-like protein FtsZ and the actin-like protein MreB.

ParM, actin and microtubule filaments all display distinct patterns of growth and shrinkage that are determined by a few key parameters and are tuned to perform specific functions. In addition, the dynamic behaviour of actin and microtubules is strictly regulated in the cell by a family of cofactors. This prevents spontaneous assembly and disassembly of filaments and enables a greater range of structural arrangements, as well as allowing the formation of the stable structures that are required as tracks for motor proteins. The parameters that determine the dynamic patterns of growth and shrinkage (and which are modulated by cofactors for actin and microtubules) include: the dissociation constants of the filament subunits in different nucleotide states; the rates of NTP hydrolysis and inorganic phosphate (P_i) release in both free and polymerized subunits; and the intrafilament stimulatory effect of adjacent NTP-bound, NDP-bound or NDP– P_i -bound subunits on those NTP hydrolysis and P_i release rates.

Dynamics of *ParM* filaments. Despite a similar overall arrangement, the dynamics of *ParM* filaments differ from the dynamics of actin filaments in several

Box 1 | Other bacterial DNA segregation systems

Type I (ParA-based) systems

The ParA-driven family of segregation systems is characterized by a deviant Walker A motif that is structurally related to the *Escherichia coli* cell division protein MinD^{60,61}; this family of proteins is known as the WACA protein family⁶². ParA systems seem to be more prevalent than the ParMRC-like actin-based systems and are similar to the widespread Soj–Spo0J system that acts in concert with several other DNA-binding proteins to regulate bacterial chromosome replication and segregation^{63–65}. These systems are composed of a motor protein (ParA), an adaptor (ParB), and a centromere (*parS*), although the names of the components differ for some systems. Typically, ParB forms a large nucleoprotein complex with *parS*^{47,66–70}, analogous to the ParR–*parC* complex of the ParMRC system. The exact mechanism by which the ParA motor protein achieves equal repositioning of ParB–*parS*-bound plasmids is not fully understood and seems to vary between different systems, but it probably requires regulated assembly of the ParA filaments over the surface of the nucleoid^{71–73}. Several ParA-like proteins have been shown to form ATP-dependent and DNA-dependent polymers that are likely to be required for DNA segregation^{71,73–80}. The most intuitive model so far for ParA-driven plasmid repositioning comes from the ParABS system of pB171 and involves pulling ParB-bound plasmids behind depolymerizing ParA filaments to achieve equal redistribution of plasmid clusters over the surface of the nucleoid⁵⁵.

Type III (TubZ-based) systems

In addition to the ParM and ParA segregation systems, a third family has recently been described that is based on a tubulin- and FtsZ-like protein, TubZ⁸¹, and which is required for the segregation of two *Bacillus subtilis* plasmids, pBT_{tox} and pXO1 (REFS 81–84). This exciting discovery highlights and reinforces the principle that segregation machineries can adopt and adapt different cytomotive filaments to achieve the same basic DNA partitioning function. Again, the TubZ system uses a predicted small DNA-binding protein, TubR, as well as a putative centromere region, and it is likely that these components will form a plasmid-bound nucleoprotein complex to couple the DNA to the filaments. In a further twist to the remarkable adaptability of cytomotive filaments, TubZ filaments differ from tubulin, exhibiting an actin-like treadmilling movement in both *B. subtilis* and *E. coli* cells and apparently forming double-helical filaments. TubZ treadmilling is reminiscent of the non-actin-like dynamic properties of ParM and shows that these basic subunit structures have been used as a scaffold to which modifications have been applied to alter a few key dynamic parameters, resulting in dynamically distinct filaments that are tuned to perform novel functions.

important ways¹⁸ (TABLE 1). ParM, actin and microtubule filaments have structural polarity, as subunits in the filaments are all arranged in the same direction. However, whereas actin and microtubules exhibit distinct kinetic properties at both ends, ParM is kinetically apolar and exhibits equal elongation from both ends^{18,19}. This is probably required to enable the ParM filaments to move plasmids in both directions, to the opposite poles of the cell. By contrast, spontaneous polymerization of both actin and microtubule filaments occurs preferentially at only one end, and this is facilitated in the cell by orientation-dependent assembly cofactors that tightly regulate unidirectional growth.

Microtubules and ParM filaments exhibit different patterns of growth and shrinkage from actin owing to differences in the dissociation rate constants of NDP-bound ends and NTP-bound ends (TABLE 1). For both microtubules and ParM, NDP-bound subunits dissociate rapidly from the ends of the filaments^{18,20}. Thus, if the filaments are not protected by an NTP-bound cap (or an additional cofactor protein), they fall apart rapidly in a behaviour known as catastrophic disassembly^{18,20}. By contrast, ADP-bound actin filaments are more stable and dissociate slowly unless assisted by an additional cofactor protein such as cofilin²¹.

Both actin and ParM assemble by a nucleation and condensation reaction, which begins with the formation of a small and stable filament nucleus and proceeds with elongation from this seed. Following nucleation, the elongation rates of ParM and of actin filaments (at the barbed end) are comparable (TABLE 1), and the key difference that defines the propensity for spontaneous polymerization is the rate of nucleation, which is 300-fold higher in ParM than in actin¹⁸. This kinetic barrier ensures that cellular actin only polymerizes at a specific time and place. By contrast, the low nucleation barrier of ParM, combined with catastrophic disassembly, enables short filaments to form spontaneously in cells and to randomly search the cell space for plasmid-bound ParR–*parC* complexes¹⁰. It is worth noting that the nucleation rate is not related to the critical concentration, which describes the minimum concentration required for bulk filament formation. The measured critical concentration of ParM is higher than that of actin (2.3 μM compared with 0.1 μM), mainly as a result of the effects of depolymerization through dynamic instability, although this critical concentration remains much lower than the estimated cellular ParM concentration (12–14 μM).

Structure of ParM. The sequence identity between actin and ParM is low (<15%), although the two proteins are of similar sizes and share a conserved patch of residues around the nucleotide-binding active site, which was originally used to predict that ParM might be an actin-like protein^{22,23}. This relationship was confirmed by the crystal structure of ParM, which revealed a fold and domain arrangement very similar to that of globular actin (G-actin)²⁴ (FIG. 2a). There are several actin-like proteins in bacteria²⁵, many of which also have low sequence identities with actin and with one another. These include filament-forming proteins such as the widespread chromosomally encoded actin homologue MreB^{26–28}, as well as the rare magnetosome-positioning protein MamK from magnetotactic bacteria^{29,30}.

The actin fold of ParM is composed of two domains, I and II, on either side of a nucleotide-binding pocket. Each of these domains is divided into two subdomains: Ia and IIa are the two larger subdomains, which share a common fold and are generally well conserved, and Ib and IIb are the two smaller subdomains, of which Ib is highly variable. Monomeric ParM has been crystallized in several different nucleotide-bound states^{24,31}, and these data have shown that the monomer undergoes a conformational change on nucleotide binding, such that the two main domains, I and II, move towards one another and close the interdomain pocket (FIG. 2b).

ParM assembles into polar, twisted, double-stranded filaments that have a general rise and twist very similar to that of F-actin, although the protofilaments wrap around one another in a left-handed arrangement in ParM compared with the right-handed organization of the protofilaments of actin^{24,31–33} (FIG. 2c–e; TABLE 1). Two parallel protofilaments wrap around each other, with $2 \times \sim 12$ subunits per complete turn in ParM compared with $2 \times \sim 13$ subunits per complete turn in actin. By contrast, protofilaments of the chromosomally encoded actin

Cofilin

Actin-binding protein that promotes disassembly at the minus ends of actin filaments.

Barbed end

The plus end of the polar F-actin polymer, which is more active than the minus end with regard to the incorporation of G-actin into the polymer.

Magnetosome

Unique intracellular structure that is found in magnetotactic bacteria and comprises a magnetic mineral crystal surrounded by a lipid bilayer membrane.

Table 1 | The structural and dynamic properties of ParM and actin filaments

Property	ParM	Actin
Structural parameters		
Protofilaments	Double, parallel and twisted ²⁴	Double, parallel and twisted ³⁵
Handedness	Left ^{31,32}	Right ³⁵
Protofilament repeat	49 Å ²⁴	55 Å ⁸⁹
Crossover repeat	~300 Å ²⁴	~360 Å ⁸⁹
Subunit repeat	~12 (REF. 24)	~13 (REF. 89)
Rotation	-165.6° (REF. 24)	166.2° (REF. 89)
Kinetic parameters		
Critical concentration (ATP)	2.3 μM ¹⁸	0.1 μM ¹⁸
Critical concentration (ADP)	~100 μM ¹⁸	1 μM ¹⁸
ATP-bound monomer association rate	4 to 5.3 μM ⁻¹ s ⁻¹ (REF. 18)	Barbed end: 10 μM ⁻¹ s ⁻¹ Pointed end: 1 μM ⁻¹ s ⁻¹ (REF. 18)
ADP-bound monomer dissociation rate	64 s ⁻¹ (REF. 18)	Barbed end: 7.2 s ⁻¹ Pointed end: 0.2 s ⁻¹ (REF. 18)
Nucleus size	3 monomers ¹⁸	3 monomers ¹⁸
Relative nucleation rate	×300 (REF. 18)	×1 (REF. 18)

homologue MreB do not twist around one another to form double filaments but rather assemble into straight double protofilaments^{28,34}.

Structural basis of dynamic behaviour. An understanding of the molecular mechanisms of filament dynamics requires a detailed comparison of the subunit conformations in different nucleotide-bound states as well as in both monomeric and filamentous arrangements. Crystal structures of filaments are difficult to obtain, and the best example comes from the chromosomally encoded bacterial actin homologue MreB, owing to fortuitous crystal packing of these filaments²⁸. MreB subunits crystallized as a protofilament, revealing the details of the longitudinal contacts, which are formed by a patch of mainly hydrophobic residues. A model of filamentous actin was first described using an electron microscopy (EM) reconstruction³⁵, and this has since been refined using X-ray fibre diffraction^{36,37}. These recent experiments predict that actin undergoes a domain rotation within each monomer to produce a thinner molecule that packs better in a filament and to also bring a key residue (glutamine 137) closer to the nucleotide-binding site.

There are currently no high-resolution structures of polymerized ParM, although several models have been described from EM reconstructions and X-ray fibre diffraction^{24,31–33}. Early discrepancies in the literature have been resolved, and it is now agreed that ParM subunits in filaments are probably mainly arranged in a closed conformation^{31,33}. Neither of the two current models^{31,33} is of sufficiently high resolution to trace the protein backbone directly, and both models used rigid-body domain movements to fit the known crystal structures. Therefore, the exact conformation of ParM in the filament is still mostly unknown.

The exact conformation of the monomers in cyto-motive filaments is important, as it helps to explain why some filaments exhibit bipolar elongation, whereas others preferentially elongate at one end. The closer the monomeric conformation is to the conformation in the filament, the more likely the filament is to elongate equally at both ends. This is because, if the subunit conformations are similar, the interface between the bottom of an incoming monomer and the top of the filament will be very similar to the interface between the top of an incoming monomer and the bottom of a filament, and therefore equal bipolar growth would be expected. Interestingly, the recent F-actin model posits a large domain rotation on polymerization, and this might explain how the subunits in F-actin are distinguished from G-actin subunits and, thus, how the two ends are kinetically distinguished^{21,36,37}.

Catastrophic disassembly requires that filament ends which are not capped by an NTP-bound subunit are only weakly bound to the previous subunit and therefore fall apart readily. It is not known whether the terminal subunits that trigger disassembly are bound to NDP-P_i or NDP, or whether they are nucleotide-free. One recent EM reconstruction found that ParM subunits in the filament were in one of two conformations — open or closed — and it was suggested that the open conformation might represent ADP-P_i-bound subunits that would undergo disassembly³³. However, it is not clear whether such a large conformational change is actually required to destabilize the filament, and the charge difference resulting from releasing, or even merely cleaving, the terminal phosphate might be sufficient to switch the intersubunit interaction from favouring assembly to favouring release.

Recently, the structure of ParM from plasmid pSK41 was determined¹². The monomeric crystal structure revealed that it was very similar to that of R1-encoded ParM, although there were some differences in the longitudinal subunit interfaces, which were confirmed by mutagenesis. Surprisingly, filaments that were assembled in the presence of different nucleotides and studied by negative-stain EM revealed bundles of filaments that the authors concluded were composed of single rather than double filaments; the mechanistic implications of this remain to be determined.

Higher-order filament structures: ParM bundles.

R1-encoded ParM filaments assemble into small bundles both in the cell, as shown by cellular cryo-EM³⁸ (FIG. 2f) and fluorescent light microscopy³⁹, and in the presence of crowding reagents *in vitro*^{38,40}. This arrangement is likely to result in stiffer structures, which may be required to move the large cargo of plasmid DNA. Unlike actin filament bundles, ParM filaments readily assemble into tightly packed bundles and do not require any additional cross-linking proteins for bundle formation. This is probably facilitated by the fact that ParM filaments contain ~12 subunits per complete turn compared with ~13 subunits per complete turn in actin. Viewed from above, this means that ParM filaments exhibit both three-fold and four-fold symmetry, allowing adjacent filaments to pack into either hexagonal or

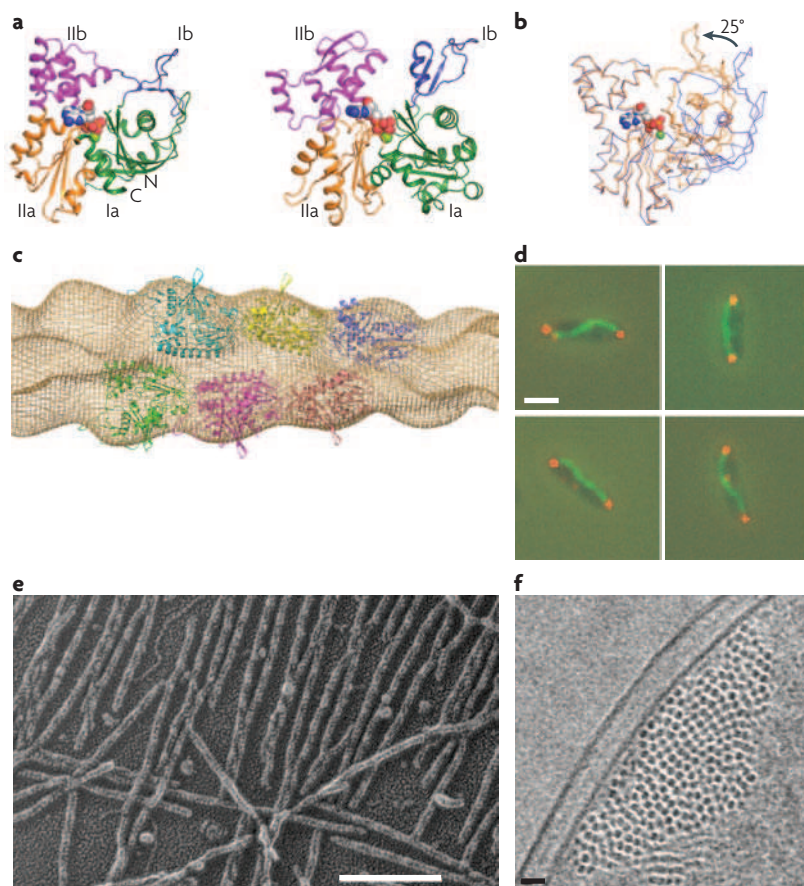


Figure 2 | The structure and properties of ParM. **a** | The monomeric structures of ParM-ADP (left; [Protein Data Bank \(PDB\)](#) accession 1MWM²⁴) and actin-ATP (right; PDB accession 1YAG⁸⁸), showing the four domains in each, Ia, Ib, IIa and IIb. The nucleotide (coloured by element) and bound magnesium (green) are shown. **b** | An overlay of the crystal structures of ParM in the apo-form and the ADP-bound form (PDB accessions 1MWK and 1MWM, respectively²⁴), showing that a domain rotation of 25° occurs on nucleotide binding. **c** | A low-resolution reconstruction of the ParM filament. Individual monomers fitted in the map are shown in a ribbon representation. **d** | Immunofluorescence micrographs of *Escherichia coli* carrying a plasmid encoding the R1 ParMRC system. ParM is stained in green and was visualized using ParM-specific antibodies. Plasmids are shown in red and were labelled using the lactose operon *LacI-lacO* marker system (see main text, BOX 1). The scale bar represents 1 μm. **e** | A quick-freeze deep-etch electron micrograph of an AMP-PNP-assembled ParM filament. The scale bar represents 100 nm. **f** | A cryo-electron micrograph of a bundle of ParM filaments viewed end on in a thin section of a rapidly frozen *E. coli* cell that was artificially induced to express high levels of ParM. There is no ParR or *parC* present. The scale bar represents 20 nm. C, carboxyl terminus; N, amino terminus. Part **d** image is reproduced, with permission, from REF. 9 © (2003) Cell Press. Part **e** image is reproduced, with permission, from REF. 32 © (2007) Macmillan Publishers Ltd. All rights reserved. Part **f** image is reproduced, with permission, from REF. 38 © (2009) American Association for the Advancement of Science.

square arrays. ParM filament bundles are thought to be composed of filaments arranged in a mixed parallel and antiparallel arrangement⁴⁰.

The adaptor complex: ParR-*parC*

Structure and arrangement of the ParR-*parC* nucleoprotein complex. ParR is a small adaptor protein of about 13 kDa that binds to a series of repeats (ten of 11 bp each in plasmid R1) in *parC*, the centromeric region of the plasmid⁴¹⁻⁴³. The crystal structure of ParR reveals an

intimate dimer with a ribbon-helix-helix dimer (RHH₂) DNA-binding domain at the amino terminus and a disordered carboxy-terminal tail^{11,13}. Multiple ParR dimers assemble into a solenoid, or open helix structure, with the DNA wrapped around the outside and the C-terminal tails, which are known to interact with ParM^{44,45}, facing into the centre (FIG. 3a). This arrangement was first suggested on the basis of crystals in which adjacent dimers packed closely together to form a continuous helix through the crystal¹³, and it was demonstrated again when ParR from pSK41 was co-crystallised with *parC* DNA and the N-terminal domains of two adjacent ParR dimers were found to be bound to 20 bp of the *parC* motif (that is, two *parC* repeats of 10 bp each)¹¹. The biological relevance of this arrangement is supported by biochemistry and EM data^{11,13}.

The exact size and arrangement of the *parC* site varies among ParMRC systems, but it is commonly positioned close to or surrounding the promoter for the downstream *parM*- and *parR*-coding region (FIG. 1a). Thus, in binding to *parC* and forming a nucleoprotein segregation complex, ParR performs a second role as a transcriptional repressor for both itself and ParM. This dual function is a typical characteristic of plasmids, which are under evolutionary pressure to keep their genomes as small as possible, and the use of DNA-binding segregation proteins as transcriptional autorepressors has been described in almost all plasmid segregation systems studied to date⁴⁶⁻⁴⁹.

Given that multiple copies of ParR bind to a series of DNA repeats, it is possible that two closely positioned *parC* regions might be coupled through cross-binding of ParR assemblies. Indeed, it has been shown that DNA molecules can be paired through their ParR-*parC* complexes *in vitro*^{13,43}. It is known that newly replicated plasmids are paired at the centre of the cell before segregation^{9,39} and that plasmids are actually segregated not as pairs of individual plasmids but as pairs of clusters of plasmids^{9,39,50}. Thus, pairing or clustering of plasmids may be achieved or facilitated through coupling of ParR-*parC* complexes, although other factors such as concatenation of newly replicated plasmids are also likely to play a part.

Interaction between ParM and the ParR-*parC* complex.

The plasmid-bound ParR-*parC* nucleoprotein complex binds to the ends of ParM filaments and protects them from catastrophic disassembly. Filaments stabilized in this way continue to polymerize with the addition of new ParM subunits at both ParR-*parC*-capped ends, although the actual rate of elongation of an individual stabilized filament is not faster than that of a non-stabilized filament^{10,18,39}. The ParR-*parC* cap simply prevents the stochastic switch from elongation to shortening that is characteristic of unprotected ParM filaments¹⁸.

The mechanism by which ParM filaments are stabilized by the plasmid-bound ParR-*parC* complex is one of the major outstanding questions in our understanding of the ParMRC segregation system. The problem can be considered in two parts: what is the structure of the tripartite ParM-ParR-*parC* complex, and how

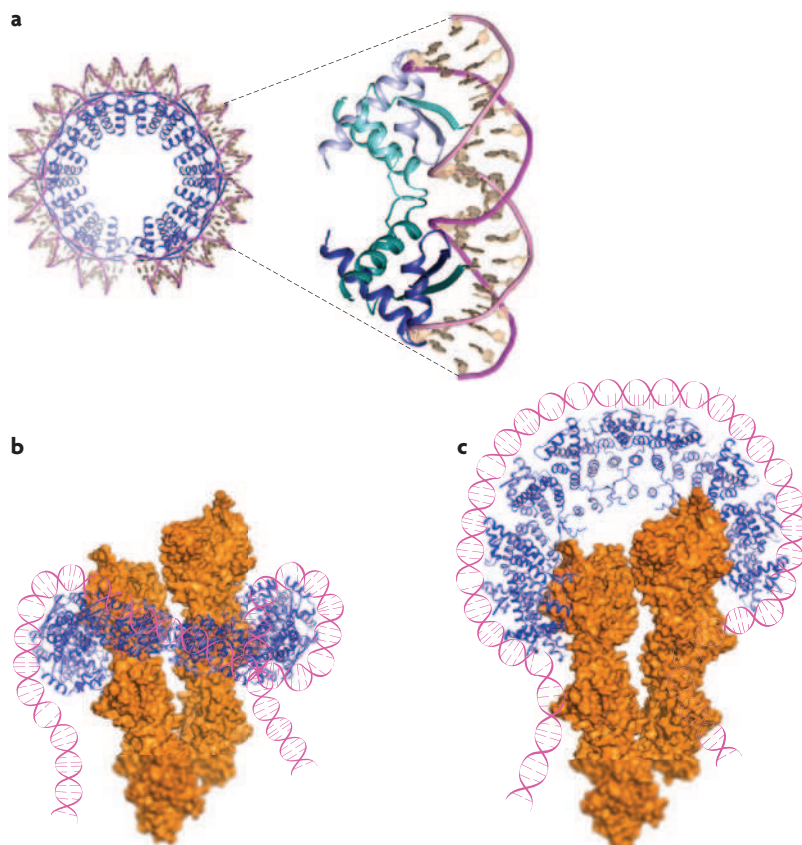


Figure 3 | The ParR-*parC* complex and its interaction with ParM filaments. **a** | The crystal structure of the ParR-*parC* complex from plasmid pSK41 ([Protein Data Bank](#) (PDB) accession 2Q2K¹¹). The DNA wraps around the outside of the open helix formed by ParR and makes contact with the ribbon-helix-helix dimer (RHH₂) DNA-binding fold of the ParR dimer¹¹. **b,c** | The 'wrap-around' model (part **b**) and the 'open-clamp' model (part **c**) for the interaction between the ParR-*parC* complex (blue and pink) and the ParM filament (orange). The ParM filament is from plasmid R1, and the ParR-*parC* complex is from plasmid pB171 (PDB accession 2JD3 (REF. 13)).

does the formation of this complex alter the behaviour of ParM filaments and protect them from dynamic instability?

The structures of both the ParR-*parC* complex and the ParM filaments are known, at least to a first approximation, and the answer to the first puzzle lies in determining how these two large oligomeric assemblies interact with one another. EM studies revealed that a single ParR-*parC* complex interacts with the very tip of a single ParM double filament^{44,45} and, further, that the ParR-*parC* complex can bind to either end of the ParM filament^{44,45}. Given that double-stranded ParM filaments are assembled in a parallel fashion and are therefore asymmetrical, the ParR-*parC* complex must somehow be able to interact with two ends that have opposite orientations.

There are two possible ways in which a solenoid structure might get around this problem, and these are reflected in the two current models for the ParMRC complex (FIG. 3b,c). In the first model, the open helix of ParR-*parC* is wrapped tightly around the ParM filament, with the C-terminal tails facing in towards the ParM filament¹¹ (FIG. 3b). In this arrangement, the ParR-*parC*

complex could adopt the same orientation with respect to the filament at either end, and the overall ParM-(ParR-*parC*)₂ structure would have polarity. A mechanism must exist to ensure that the ParR-*parC* complex stays associated with the elongating filament ends, and this could be achieved through a preference for binding ATP-ParM over ADP-ParM, which has been shown experimentally⁴⁴. The advantage of this 'wrap-around' model is that it solves the polarity problem, but the disadvantage is that it is questionable whether there is enough space in the pore of ParR-*parC* to hold the ParM filament. In the second model for the ParMRC complex, the ParR-*parC* complex is proposed to form a clamp that sits at the very end of the ParM filament and holds the filament tip in its jaw⁴⁴ (FIG. 3c). In this 'clamp' model, the orientation of the ParR-*parC* complex with respect to the filament would be opposite at either end of the filament, and this would require that the C-terminal tails of ParR bind to the sides of the filament with a flexibility that would allow the two opposite orientations to be accommodated. This is not a major theoretical problem, as the connecting loop between the main part of ParR and the putative ParM-binding helix is disordered and will therefore be able to easily rotate through the necessary 180° to reorient the helix at either end of the filament.

The answer to the second, related puzzle lies in understanding the molecular mechanism by which the ParR-*parC* complex stabilizes ParM filaments and, thus, protects them from disassembly. This is difficult to determine, as there are several possible individual components, the contributions of which cannot easily be measured in isolation. These components include: physically protecting the ends from disassembly; inducing a conformational change in ParM such that the terminal subunit is in a filament-binding conformation; directly or indirectly inducing nucleotide hydrolysis; and adding binding energy for the incoming ParM subunits. Both the wrap-around model and the clamp model of the ParMRC complex postulate that the ParR ring contacts the ends of the ParM filament at two points, which would mechanically protect the ends of the filament from disassembly. Each ParR-*parC* complex contains approximately 20 C-terminal ParR tails, which are disordered in solution and are known to mediate the interaction with ParM^{44,45}. Two or more of these tails may become ordered on interaction with the ParM filament and, in addition to stabilizing the ParM-(ParR-*parC*) interaction, this may induce a conformational change in ParM that favours filament formation. It is known that the interaction of the filament with ParR-*parC* also leads to an increase in nucleotide hydrolysis, as measured by an increase in the rate of P_i release^{30,51}, although it is unclear whether this is a direct effect (for example through stimulation by the ParR tails) or whether this measurement simply reflects the increase in polymerization, which in turn leads to higher bulk rates.

The ParMRC complex in the cell

Movement of plasmid DNA to opposite poles of the cell proceeds in a cyclic manner that is uncoupled from the host cell cycle and that has been observed in detail by

Box 2 | Imaging the ParMRC system by light microscopy

Fluorescence light microscopy has provided some of the most important insights into the ParMRC system. Immunofluorescence images showing pole-to-pole filaments of ParM capped by plasmids at either end led to the hypothesis that ParM separates plasmids to the cell poles by a dynamic, mitotic-like mechanism⁹ (see main text, FIG. 2d). Immunofluorescence light microscopy has been used to label ParM and plasmids, and it has the important advantage that it is carried out on fixed cells and therefore does not interfere with dynamic function, although serious artefacts can be introduced during the fixation process. Live-cell microscopy has the great advantage that it can be used to follow dynamic processes in real time and on native cells, but it suffers the risk of perturbing function through the use of fluorescent labels and markers.

Labelling plasmid DNA

The lactose operon *lacI-lacO* system was first developed for yeast⁸⁵ and has since been widely used in various designs to label plasmid and chromosomal DNA in both fixed and living bacterial cells^{86,87}. The basic principle in its original form is as follows. The DNA-binding protein *lacI* is expressed at low levels as a fluorescent fusion protein (fused, for example, to GFP) from an expression plasmid. Many repeats (40–256 copies) of the *lacI* binding site, *lacO*, are introduced into the DNA of interest (for example, the ParMRC-carrying R1 plasmid). *lacI*-GFP binds to this large region of DNA and thus illuminates the DNA molecule. This technique has been used to monitor plasmid and chromosome dynamics in living cells, and GFP-specific antibodies have been used to enhance the signal for immunofluorescence microscopy. The drawback of this approach is that the large additional region of DNA and the weak dimerization of GFP may affect the replication and segregation of the target DNA molecule, as has recently been shown for the low-copy-number plasmid P1 (REF. 54).

Labelling ParM

Filamentous proteins are notoriously difficult to engineer as functional fusion proteins owing to the extensive longitudinal and lateral interactions, and ParM, with its additional requirement to bind to ParR-*parC*, has been no exception. As one solution to this problem, Campbell and colleagues constructed a non-functional mCherry-ParM fusion protein and used this protein at very low levels to visualize wild-type, plasmid-segregating ParM filaments³⁹. In the most comprehensive live-cell microscopy study of the ParMRC system to date, this approach was combined with *lacI-lacO* technique to simultaneously track the progression of both plasmids and ParM filaments in live cells. By contrast, a fusion protein featuring GFP and the actin- and ParM-like filament Alp7A was apparently functional, as determined by complementation. In this case, the dynamics of these fully labelled, plasmid-segregating dynamic filaments were tracked in live cells¹⁴.

fluorescence light microscopy (BOX 2; FIG. 2d)^{9,39,51}. ParM filaments polymerize bidirectionally in a small bundle, with clusters of plasmids attached to either end of the bundle. On reaching the ends of the cell, the ParM filament disassembles and the plasmids remain anchored at the cell poles for some time before diffusing away throughout the cell. When two plasmid foci encounter each other, they remain associated for some time before ParM filaments form between them again, pushing them to the opposite poles of the cell; thus, the cycle begins once more³⁹.

Questions remain about exactly what happens in paired plasmid clusters at the point of segregation initiation. The copy number of the R1 plasmid is 4–6 (REF. 52), but these copies are usually located in a lower number of discrete clusters in the cell⁵⁰. Given that one ParM filament can interact with one ParR-*parC* complex at each end^{44,45}, it might be predicted that pairs of clusters of replicated plasmids would be separated by bundles of a roughly equal number of ParM filaments. Indeed, EM of thin sections of *E. coli* cells carrying a miniature version of plasmid R1 revealed small bundles of 3–5 ParM filaments each³⁸. However, it is possible that only one or a

few of the filaments in the bundle are actually attached to plasmids, with the rest being stabilized simply by their presence in the bundle. As described above, it has been proposed that ParM filaments use dynamic instability to search the cell space for ParR-*parC* complexes¹⁰. But what happens when a ParM filament locates a ParR-*parC* complex at both ends? It may form a stable, primed complex that waits for all ParR-*parC* complexes to pair up with ParM filaments in a mitotic-like composition. In this case, two plasmid clusters would be linked until all plasmids were paired by short ParM filaments, at which point a trigger would be required to release the plasmids and permit stable elongation of the filament bundle. Alternatively, there may be no bulk control system, and the stabilization of one or a few ParM filaments may be sufficient to drive segregation, although in this scenario the number of plasmids that is moved to either end of the cell might be more variable.

The ParMRC segregation system moves plasmids to the very ends of the cell, close to the cell poles and beyond the end of the nucleoid^{10,39,50}. This is in contrast to most other plasmid segregation systems as well as many bacterial chromosomal segregation systems, which move their DNA to approximately the quarter-cell positions that mark the edge of the nucleoid^{53–55}. The pole positioning of the ParMRC system is not dependent on the origin of replication, as it was also observed when the ParMRC system was moved onto a mini F-plasmid, which normally localizes to the quarter-cell position^{9,39}. It is not known whether a host cell-encoded factor is required to tether the plasmids to the cell poles, or whether this localization simply reflects the fact that ParM filaments will continue to grow until they are stopped by the boundaries of the cell. It is also not clear what triggers ParM depolymerization and plasmid release on completion of segregation.

Other ParMRC-like segregation systems

The basic principle of using a cytomotive-filament-forming actin-like protein to move DNA to the opposite poles of the cell has been adopted by several plasmid segregation systems across the Bacteria^{14,15} (TABLE 2). These systems are not closely related in sequence and could only be identified by multiple rounds of BLAST searches based on the small actin signature motif that lines the nucleotide-binding pocket¹⁴. However, low sequence identity does not necessarily mean that these systems evolved independently, as plasmid genes can evolve much more rapidly than those on the chromosome. On the basis of the few systems that have been examined in detail, it seems that the extended family of bacterial actin-like proteins is characterized by a common fold in the monomers, which assemble into cytomotive filaments to segregate plasmid DNA, although there are some apparent differences in the exact mechanism by which this is achieved^{16,17}.

The first ParMRC-like plasmid segregation system to be studied in detail was the AlfaB system from the *Bacillus subtilis* plasmid pBET131¹⁵. Alfa is only distantly related to ParM and actin, but it also forms dynamic filaments that achieve segregation of a

Nucleoid

Distinct region in the bacterial cytoplasm that harbours the chromosomal DNA.

Formin

Protein that contains a formin homology 2 (FH2) domain and promotes actin assembly. Formin binds to the ends of actin filaments.

Table 2 | **Selected bacterial proteins involved in DNA or organelle movement**

Protein	Type	Protein family	Function	Encoded by
ParM	Cytomotive filament	Actin	Plasmid segregation	R1, pSK41 and pB171
ParR	Adaptor protein	DNA-binding	Plasmid segregation	R1, pSK41 and pB171
AlfA	Cytomotive filament	Actin	Plasmid segregation	pBET131
AlfB	Adaptor protein	DNA-binding	Plasmid segregation	pBET131
Alp7A	Cytomotive filament	Actin	Plasmid segregation	pLS20
TubZ	Cytomotive filament	Tubulin	Plasmid segregation	pBtoxis and pXO1
TubR	Adaptor protein	DNA-binding	Plasmid segregation	pBtoxis and pXO1
ParA	Cytomotive filament	Deviant Walker A	Plasmid segregation	P1, F, pB171, TP228 and others
ParB	Adaptor protein	DNA-binding	Plasmid segregation	P1, F, pB171, TP228 and others
MinD	Cytomotive filament	Deviant Walker A	Identification of mid-cell position	Chromosome
MreB	Cytomotive filament	Actin	Major component of the bacterial cytoskeleton, involved in cell shape and organization	Chromosome
MamK	Cytomotive filament	Actin	Positioning of magnetic organelles	Chromosome
FtsZ	Cytomotive filament	Tubulin	Major component of the bacterial cytoskeleton, involved in Z ring assembly and cell division	Chromosome

low-copy-number plasmid. AlfA is encoded together with a small protein, AlfB, which is essential for segregation and has been shown to carry out similar centromere-binding and gene regulation activities to ParR⁵⁶. *In vitro* analysis of purified AlfA revealed bundles of parallel filaments that were much more twisted than their ParM or actin counterparts, and the AlfA monomers polymerized more readily than either ParM or actin^{16,17}. Two separate studies found that there was no evidence of dynamic instability *in vitro*^{16,17}, and these filaments might use a novel mechanism to achieve DNA segregation, such as unidirectional extrusion of one of a pair of plasmids from one pole.

Another actin-like, plasmid-encoded protein, Alp7A, was identified from plasmid LS20 of *B. subtilis* subsp. *natto* and found to assemble into dynamic filaments that are required for plasmid segregation¹⁴. Fluorescently labelled Alp7A was shown to undergo cycles of rapid growth and shrinkage in a pattern strongly reminiscent of R1-encoded ParM. Using photobleaching, it was further shown that seemingly static filaments that extended from pole to pole also underwent dynamic turnover, with unidirectional growth into a photobleached spot, suggesting a treadmilling motion that has not previously been reported for ParM.

Key remaining questions

ParMRC remains one of the best characterised systems for DNA segregation. The structures and organization of the individual components have been determined,

and we have a general overview of how these components come together to achieve DNA motility. At the molecular level, the biggest outstanding puzzle is exactly how the large ParR–*parC* complex interacts with and stabilizes the ends of ParM filaments. This is not a trivial problem. Definitive structural analysis will require high-resolution details of both the ParM filament and the ParMRC tripartite complex. Despite over 50 years of study, detailed structural information on the conformation of filamentous actin has only recently been obtained through X-ray fibre diffraction³⁷. In addition, a complete mechanistic understanding will require biophysical analysis of the ParR–*parC*-induced protection from dynamic instability; the analogous problem of formin-mediated actin stabilization remains, for the most part, unresolved.

In the long term, the major challenge for ParMRC research will be to understand plasmid segregation in the cellular environment, where DNA segregation must contend with the effects of competing processes such as DNA replication, transcription, supercoiling, concatenation and conjugation. Emerging high-resolution techniques in both EM and light microscopy are beginning to allow us to image and track individual molecules in cells and are revealing a complex and highly dynamic view of the subcellular assemblies in bacteria^{57–59}. Plasmid segregation systems make ideal models for applying these techniques, and it will be exciting to see what can be learned about DNA motility in the complex and crowded native environment of the cell.

1. Ebersbach, G. & Gerdes, K. Plasmid segregation mechanisms. *Annu. Rev. Genet.* **39**, 453–479 (2005).
2. Ghosh, S. K., Hajra, S., Paek, A. & Jayaram, M. Mechanisms for chromosome and plasmid segregation. *Annu. Rev. Biochem.* **75**, 211–241 (2006).
3. Schumacher, M. A. Structural biology of plasmid partition: uncovering the molecular mechanisms of DNA segregation. *Biochem. J.* **412**, 1–18 (2008).

4. Gerdes, K., Howard, M. & Szardenings, F. Pushing and pulling in prokaryotic DNA segregation. *Cell* **141**, 927–942 (2010).
5. Löwe, J. & Amos, L. A. Evolution of cytomotive filaments: the cytoskeleton from prokaryotes to eukaryotes. *Int. J. Biochem. Cell Biol.* **41**, 323–329 (2009).

6. A description of nucleotide-driven dynamic filaments as 'cytomotive filaments', and a discussion of the evolutionary and mechanistic implications. Ni, L., Xu, W., Kumaraswami, M. & Schumacher, M. A. Plasmid protein TubR uses a distinct mode of HTH-DNA binding and recruits the prokaryotic tubulin homolog TubZ to effect DNA partition. *Proc. Natl Acad. Sci. USA* **107**, 11763–11768 (2010).

7. Simpson, A. E., Skurray, R. A. & Firth, N. A single gene on the staphylococcal multiresistance plasmid pSK1 encodes a novel partitioning system. *J. Bacteriol.* **185**, 2143–2152 (2003).
8. Gerdes, K., Larsen, J. E. & Molin, S. Stable inheritance of plasmid R1 requires two different loci. *J. Bacteriol.* **161**, 292–298 (1985).
9. Møller-Jensen, J. *et al.* Bacterial mitosis: ParM of plasmid R1 moves plasmid DNA by an actin-like insertional polymerization mechanism. *Mol. Cell* **12**, 1477–1487 (2003).
The first immunofluorescence images showing labelled cellular ParM filaments and labelled plasmids. The filaments run along the length of the cell, with plasmids at both ends. This is also the first description of an insertional polymerization mechanism.
10. Garner, E. C., Campbell, C. S., Weibel, D. B. & Mullins, R. D. Reconstitution of DNA segregation driven by assembly of a prokaryotic actin homolog. *Science* **315**, 1270–1274 (2007).
The entire ParMRC complex is reconstituted *in vitro*, and ParM filaments are seen to move ParR–parC-bound polystyrene beads apart. This is also the first description of the ‘search and capture’ mechanism.
11. Schumacher, M. A. *et al.* Segosome structure revealed by a complex of ParR with centromere DNA. *Nature* **450**, 1268–1271 (2007).
The co-crystal structure of pSK41-encoded ParR and short fragments of parC DNA, showing parC bound to the RHH₁ surface on the outside surface of the ParR helix.
12. Popp, D. *et al.* Structure and filament dynamics of the pSK41 actin-like ParM protein: implications for plasmid DNA segregation. *J. Biol. Chem.* **285**, 101300–101340 (2010).
13. Møller-Jensen, J., Ringgaard, S., Mercogliano, C. P., Gerdes, K. & Löwe, J. Structural analysis of the ParR/parC plasmid partition complex. *EMBO J.* **26**, 4413–4422 (2007).
The first crystal structure of ParR, in which ParR alone is crystallized in a continuous helical arrangement. This study includes an EM demonstration of ParR–parC rings and an analysis of DNA binding through mutagenesis of parR.
14. Derman, A. I. *et al.* Phylogenetic analysis identifies many uncharacterized actin-like proteins (Alps) in bacteria: regulated polymerization, dynamic instability and treadmilling in Alp7A. *Mol. Microbiol.* **73**, 534–552 (2009).
15. Becker, E. *et al.* DNA segregation by the bacterial actin AlfA during *Bacillus subtilis* growth and development. *EMBO J.* **25**, 5919–5931 (2006).
16. Polka, J. K., Kollman, J. M., Agard, D. A. & Mullins, R. D. The structure and assembly dynamics of plasmid actin AlfA imply a novel mechanism of DNA segregation. *J. Bacteriol.* **191**, 6219–6230 (2009).
17. Popp, D. *et al.* Polymeric structures and dynamic properties of the bacterial actin AlfA. *J. Mol. Biol.* **397**, 1031–1041 (2010).
18. Garner, E. C., Campbell, C. S. & Mullins, R. D. Dynamic instability in a DNA-segregating prokaryotic actin homolog. *Science* **306**, 1021–1025 (2004).
The first demonstration of dynamic instability and bipolar elongation for ParM, and a detailed analysis of the dynamic properties of ParM compared with those of actin.
19. Popp, D. *et al.* Concerning the dynamic instability of actin homolog ParM. *Biochem. Biophys. Res. Commun.* **353**, 109–114 (2007).
20. Mitchison, T. & Kirschner, M. Dynamic instability of microtubule growth. *Nature* **312**, 237–242 (1984).
21. Pfäendner, J., Lyman, E., Pollard, T. D. & Voth, G. A. Structure and dynamics of the actin filament. *J. Mol. Biol.* **396**, 252–263 (2010).
22. Bork, P., Sander, C. & Valencia, A. An ATPase domain common to prokaryotic cell cycle proteins, sugar kinases, actin, and hsp70 heat shock proteins. *Proc. Natl Acad. Sci. USA* **89**, 7290–7294 (1992).
23. Jensen, R. B. & Gerdes, K. Partitioning of plasmid R1. The ParM protein exhibits ATPase activity and interacts with the centromere-like ParR–parC complex. *J. Mol. Biol.* **269**, 505–513 (1997).
24. van den Ent, F., Møller-Jensen, J., Amos, L. A., Gerdes, K. & Löwe, J. F-actin-like filaments formed by plasmid segregation protein ParM. *EMBO J.* **21**, 6935–6943 (2002).
The first crystal structure of plasmid R1-encoded ParM, and the first molecular model of ParM double filaments.
25. Carballido-Lopez, R. The bacterial actin-like cytoskeleton. *Microbiol. Mol. Biol. Rev.* **70**, 888–909 (2006).
26. Jones, L. J., Carballido-Lopez, R. & Errington, J. Control of cell shape in bacteria: helical, actin-like filaments in *Bacillus subtilis*. *Cell* **104**, 913–922 (2001).
27. van den Ent, F., Amos, L. & Löwe, J. Bacterial ancestry of actin and tubulin. *Curr. Opin. Microbiol.* **4**, 634–638 (2001).
28. van den Ent, F., Amos, L. A. & Löwe, J. Prokaryotic origin of the actin cytoskeleton. *Nature* **413**, 39–44 (2001).
29. Komeili, A., Li, Z., Newman, D. K. & Jensen, G. J. Magnetosomes are cell membrane invaginations organised by the actin-like protein MamK. *Science* **311**, 242–245 (2006).
30. Taoka, A., Asada, R., Wu, L. F. & Fukumori, Y. Polymerisation of the actin-like protein MamK, which is associated with magnetosomes. *J. Bacteriol.* **189**, 8737–8740 (2007).
31. Popp, D. *et al.* Molecular structure of the ParM polymer and the mechanism leading to its nucleotide-driven dynamic instability. *EMBO J.* **27**, 570–579 (2008).
32. Orlova, A. *et al.* The structure of bacterial ParM filaments. *Nature Struct. Mol. Biol.* **14**, 921–926 (2007).
33. Galkin, V. E., Orlova, A., Rivera, C., Mullins, R. D. & Egelman, E. H. Structural polymorphism of the ParM filament and dynamic instability. *Structure* **17**, 1253–1264 (2009).
34. Popp, D. *et al.* Filament structure, organization and dynamics in MreB sheets. *J. Biol. Chem.* **285**, 15858–15865 (2010).
35. Holmes, K., Popp, D., Gebhard, W. & Kabsch, W. Atomic model of the actin filament. *Nature* **347**, 44–49 (1990).
36. Holmes, K. Actin in a twist. *Nature* **457**, 389–390 (2009).
37. Oda, T., Iwasa, M., Aihara, T., Maeda, Y. & Narita, A. The nature of the globular- to fibrous-actin transition. *Nature* **457**, 441–445 (2009).
38. Salje, J., Zuber, B. & Löwe, J. Electron cryomicroscopy of *E. coli* reveals filament bundles involved in plasmid DNA segregation. *Science* **323**, 509–512 (2009).
A direct observation of ParM filaments in *E. coli* using cellular cryo-EM techniques.
39. Campbell, C. S. & Mullins, R. D. *In vivo* visualization of type II plasmid segregation: bacterial actin filaments pushing plasmids. *J. Cell Biol.* **179**, 1059–1066 (2007).
The first observation of dynamic ParM filaments and plasmids in live *E. coli* cells.
40. Popp, D., Narita, A., Iwasa, M., Maeda, Y. & Robinson, R. C. Molecular mechanism of bundle formation by the bacterial actin ParM. *Biochem. Biophys. Res. Commun.* **391**, 1598–1603 (2010).
41. Dam, M. & Gerdes, K. Partitioning of plasmid R1. Ten direct repeats flanking the parA promoter constitute a centromere-like partition site parC, that expresses incompatibility. *J. Mol. Biol.* **236**, 1289–1298 (1994).
42. Jensen, R. B., Dam, M. & Gerdes, K. Partitioning of plasmid R1. The parA operon is autoregulated by ParR and its transcription is highly stimulated by a downstream activating element. *J. Mol. Biol.* **236**, 1299–1309 (1994).
43. Jensen, R. B., Lurz, R. & Gerdes, K. Mechanism of DNA segregation in prokaryotes: replicon pairing by parC of plasmid R1. *Proc. Natl Acad. Sci. USA* **95**, 8550–8555 (1998).
44. Salje, J. & Löwe, J. Bacterial actin: architecture of the ParMRC plasmid DNA partitioning complex. *EMBO J.* **27**, 2230–2238 (2008).
A demonstration of the 1/1 stoichiometry between ParM filaments and the ParR–parC complex, and a description of the clamp model for ParMRC.
45. Choi, C. L., Claridge, S. A., Garner, E. C., Alivisatos, A. P. & Mullins, R. D. Protein-nanocrystal conjugates support a single filament polymerization model in R1 plasmid segregation. *J. Biol. Chem.* **283**, 28081–28086 (2008).
46. Davey, M. J. & Funnell, B. E. The P1 plasmid partition protein ParA. A role for ATP in site-specific DNA binding. *J. Biol. Chem.* **269**, 29908–29913 (1994).
47. Davey, M. J. & Funnell, B. E. Modulation of the P1 plasmid partition protein ParA by ATP, ADP, and P1 ParB. *J. Biol. Chem.* **272**, 15286–15292 (1997).
48. Davis, M. A., Martin, K. A. & Austin, S. J. Biochemical activities of the ParA partition protein of the P1 plasmid. *Mol. Microbiol.* **6**, 1141–1147 (1992).
49. Golovanov, A. P., Barilla, D., Golovanova, M., Hayes, F. & Lian, L. Y. ParG, a protein required for active partition of bacterial plasmids, has a dimeric ribbon–helix–helix structure. *Mol. Microbiol.* **50**, 1141–1153 (2003).
50. Weitaio, T., Dasgupta, S. & Nordström, K. Plasmid R1 is present as clusters in the cells of *Escherichia coli*. *Plasmid* **43**, 200–204 (2000).
51. Møller-Jensen, J., Jensen, R. B., Löwe, J. & Gerdes, K. Prokaryotic DNA segregation by an actin-like filament. *EMBO J.* **21**, 3119–3127 (2002).
The first demonstration of dynamic filament formation by ParM, and the first molecular model for ParMRC plasmid segregation.
52. Nordström, K., Molin, S. & Aagaard-Hansen, H. Partitioning of plasmid R1 in *Escherichia coli*. I. Kinetics of loss of plasmid derivatives deleted of the par region. *Plasmid* **4**, 215–227 (1980).
53. Gordon, S., Rech, J., Lane, D. & Wright, A. Kinetics of plasmid segregation in *Escherichia coli*. *Mol. Microbiol.* **51**, 461–469 (2004).
54. Sengupta, M., Nielsen, H. J., Youngren, B. & Austin, S. P1 plasmid segregation: accurate redistribution by dynamic plasmid pairing and separation. *J. Bacteriol.* **192**, 1175–1183 (2010).
55. Ringgaard, S., van Zon, J., Howard, M. & Gerdes, K. Movement and equi-positioning of plasmids by ParA filament disassembly. *Proc. Natl Acad. Sci. USA* **106**, 19369–19374 (2009).
56. Tanaka, T. Functional analysis of the stability determinant AlfB of pBET131, a miniplasmid derivative of *Bacillus subtilis* (natto) plasmid pLS32. *J. Bacteriol.* **192**, 1221–1230 (2010).
57. Greenfield, D. *et al.* Self-organization of the *Escherichia coli* chemotaxis network imaged with super-resolution light microscopy. *PLoS Biol.* **7**, e1000137 (2009).
58. Milne, J. L. & Subramaniam, S. Cryo-electron tomography of bacteria: progress, challenges and future prospects. *Nature Rev. Microbiol.* **7**, 666–675 (2009).
59. Li, Z. & Jensen, G. J. Electron cryotomography: a new view into microbial ultrastructure. *Curr. Opin. Microbiol.* **12**, 333–340 (2009).
60. Raskin, D. M. & de Boer, P. A. Rapid pole-to-pole oscillation of a protein required for directing division to the middle of *Escherichia coli*. *Proc. Natl Acad. Sci. USA* **96**, 4971–4976 (1999).
61. Cordell, S. C. & Löwe, J. Crystal structure of the bacterial cell division regulator MinD. *FEBS Lett.* **492**, 160–165 (2001).
62. Michie, K. & Löwe, J. Dynamic filaments of the bacterial cytoskeleton. *Annu. Rev. Biochem.* **75**, 467–492 (2006).
63. Lee, P. S. & Grossman, A. D. The chromosome partitioning proteins Soj (ParA) and Spo0J (ParB) contribute to accurate chromosome partitioning, separation of replicated sister origins, and regulation of replication initiation in *Bacillus subtilis*. *Mol. Microbiol.* **60**, 853–869 (2006).
64. Murray, H. & Errington, J. Dynamic control of the DNA replication initiation protein DnaA by Soj/ParA. *Cell* **135**, 74–84 (2008).
65. Gruber, S. & Errington, J. Recruitment of condensin to replication origin regions by ParB/Spo0J promotes chromosome segregation in *B. subtilis*. *Cell* **137**, 685–696 (2009).
66. Rodionov, O., Lobočka, M. & Yarmolinsky, M. Silencing of genes flanking the P1 plasmid centromere. *Science* **283**, 546–549 (1999).
67. Surtees, J. A. & Funnell, B. E. The DNA binding domains of P1 ParB and the architecture of the P1 plasmid partition complex. *J. Biol. Chem.* **276**, 12385–12394 (2001).
68. Rodionov, O. & Yarmolinsky, M. Plasmid partitioning and the spreading of P1 partition protein ParB. *Mol. Microbiol.* **52**, 1215–1223 (2004).
69. Schumacher, M. A. & Funnell, B. E. Structures of ParB bound to DNA reveal mechanism of partition complex formation. *Nature* **438**, 516–519 (2005).
70. Schumacher, M. A., Mansoor, A. & Funnell, B. E. Structure of a four-way bridged ParB–DNA complex provides insight into P1 segrosome assembly. *J. Biol. Chem.* **282**, 10456–10464 (2007).
71. Lim, G. E., Derman, A. I. & Pogliano, J. Bacterial DNA segregation by dynamic SopA polymers. *Proc. Natl Acad. Sci. USA* **102**, 17658–17663 (2005).
72. Castaing, J. P., Bouet, J. Y. & Lane, D. F plasmid partition depends on interaction of SopA with non-specific DNA. *Mol. Microbiol.* **70**, 1000–1011 (2008).
73. Bouet, J. Y., Ah-Seng, Y., Benmeradi, N. & Lane, D. Polymerization of SopA partition ATPase: regulation

- by DNA binding and SopB. *Mol. Microbiol.* **63**, 468–481 (2007).
74. Barilla, D., Rosenberg, M. F., Nobbmann, U. & Hayes, F. Bacterial DNA segregation dynamics mediated by the polymerizing protein ParF. *EMBO J.* **24**, 1453–1464 (2005).
 75. Barilla, D., Carmelo, E. & Hayes, F. The tail of the ParG DNA segregation protein remodels ParF polymers and enhances ATP hydrolysis via an arginine finger-like motif. *Proc. Natl Acad. Sci. USA* **104**, 1811–1816 (2007).
 76. Dunham, T. D., Xu, W., Funnell, B. E. & Schumacher, M. A. Structural basis for ADP-mediated transcriptional regulation by P1 and P7 ParA. *EMBO J.* **28**, 1792–1802 (2009).
 77. Ebersbach, G. *et al.* Regular cellular distribution of plasmids by oscillating and filament-forming ParA ATPase of plasmid pB171. *Mol. Microbiol.* **61**, 1428–1442 (2006).
 78. Hatano, T., Yamaichi, Y. & Niki, H. Oscillating focus of SopA associated with filamentous structure guides partitioning of F plasmid. *Mol. Microbiol.* **64**, 1198–1213 (2007).
 79. Leonard, T. A., Møller-Jensen, J. & Lowe, J. Towards understanding the molecular basis of bacterial DNA segregation. *Philos. Trans. R. Soc. Lond. B Biol. Sci.* **360**, 523–535 (2005).
 80. Suefuji, K., V. R., RayChaudhuri, D. Dynamic assembly of MinD into filament bundles modulated by ATP, phospholipids and MinE. *Proc. Natl Acad. Sci. USA* **99**, 16776–16781 (2002).
 81. Larsen, R. A. *et al.* Treadmilling of a prokaryotic tubulin-like protein, TubZ, required for plasmid stability in *Bacillus thuringiensis*. *Genes Dev.* **21**, 1340–1352 (2007).
 82. Berry, C. *et al.* Complete sequence and organisation of pBtoxis, the toxin-encoding plasmid of *Bacillus thuringiensis* subsp. *israelensis*. *Appl. Environ. Microbiol.* **72**, 5082–5095 (2002).
 83. Tang, M., Bideshi, D. K., Park, H. W. & Federici, B. A. Minireplicon from pBtoxis of *Bacillus thuringiensis* subsp. *israelensis*. *Appl. Environ. Microbiol.* **72**, 6948–6954 (2006).
 84. Tinsley, E. & Khan, S. A. A novel FtsZ-like protein is involved in replication of the anthrax toxin-encoding pXO1 plasmid in *Bacillus anthracis*. *J. Bacteriol.* **188**, 2829–2835 (2006).
 85. Robinett, C. C. *et al.* *In vivo* localization of DNA sequences and visualization of large-scale chromatin organization using lac operator/repressor recognition. *J. Cell Biol.* **135**, 1685–1700 (1996).
 86. Lemon, K. P. & Grossman, A. D. Movement of replicating DNA through a stationary replisome. *Mol. Cell* **6**, 1321–1330 (2000).
 87. Wang, X., Reyes-Lamothe, R. & Sherratt, D. J. Visualizing genetic loci and molecular machines in living bacteria. *Biochem. Soc. Trans.* **36**, 749–753 (2008).
 88. Vorobiev, S. *et al.* The structure of nonvertebrate actin: implications for the ATP hydrolytic mechanism. *Proc. Natl Acad. Sci. USA* **100**, 5760–5765 (2003).
 89. Galkin, V. E., VanLoock, M. S., Orlova, A. & Egelman, E. H. A new internal mode in F-actin helps explain the remarkable evolutionary conservation of actin's sequence and structure. *Curr. Biol.* **12**, 570–575 (2002).

Acknowledgements

The authors are grateful to K. Gerdes for helpful comments on the manuscript and to J. Møller-Jensen for ongoing collaborations.

Competing interests statement

The authors declare no competing financial interests.

FURTHER INFORMATION

Jan Löwe's homepage: <http://www2.mrc-lmb.cam.ac.uk/group-leaders/h-to-m/j-lowe>

Protein Data Bank: <http://www.pdb.org/pdb/home/home.do>

ALL LINKS ARE ACTIVE IN THE ONLINE PDF